Hindawi Publishing Corporation
International Journal of Photoenergy
Volume 2014, Article ID 724910, 9 pages
http://dx.doi.org/10.1155/2014/724910

Research Article

Sol-Gel to Prepare Nitrogen Doped TiO_2 Nanocrystals with Exposed {001} Facets and High Visible-Light Photocatalytic Performance

Hui-Ying Ai,[1] Jian-Wen Shi,[1] Rui-Xi Duan,[2] Jian-Wei Chen,[1] Hao-Jie Cui,[1] and Ming-Lai Fu[1]

[1] *Key Laboratory of Urban Environment and Health, Institute of Urban Environment, Chinese Academy of Sciences, No. 1799, Jimei Road, Xiamen, Fujian 361021, China*
[2] *China National Petroleum Offshore Engineering Co., Ltd., Beijing 100028, China*

Correspondence should be addressed to Jian-Wen Shi; shijnwn@163.com and Ming-Lai Fu; mlfu@iue.ac.cn

Received 1 April 2014; Revised 3 June 2014; Accepted 17 June 2014; Published 7 July 2014

Academic Editor: Qing Wang

A series of N-doped TiO_2 nanocrystals with exposed {001} facets was prepared successfully by sol-gel method for the first time. The physicochemical properties of these resultant photocatalysts were characterized by XRD, TEM, XPS, and DRS, and their photocatalytic performances were evaluated by photocatalytic decoloration of methylene blue solution under visible light ($\lambda > 420$ nm) irradiation. The results showed that the N-doped TiO_2 nanocrystals with exposed {001} facets showed higher photocatalytic activity than P25. The enhanced photocatalytic performance can be attributed to synergistic effects of several factors, such as good crystallinity, better light response characteristic, and high reactivity of {001} facets.

1. Introduction

TiO_2 with exposed {001} facets has attracted great attention in recent years because of its outstanding advantages in photocatalysis field [1–3], such as excellent thermodynamic stability, strong oxidizing power, and low cost. Many researchers have participated in optimizing its photocatalytic activity since the large percentage of {001} reactive facets were prepared by one-pot hydrothermal method using TiF_4 as precursor firstly [4]. It is widely believed that {001} facets of anatase TiO_2 provide more active sites for photocatalytic oxidation reaction [5, 6], so its photocatalytic activity can be improved significantly. However, the photocatalytic activity of TiO_2 is still limited by narrow light absorption (only responsive to UV with wavelength below 387 nm due to its wide band-gap) and rapid recombination of photon-generated carriers. To promote the better performance of TiO_2, anion doping, especially nitrogen doping, would be effective solution. Experiments and theories have proved that the doping of nitrogen can introduce a new impurity level in the band gap of TiO_2, which provides a springboard for electron transition and promotes the visible-light response of TiO_2 [7–9].

The popular approach to synthesize TiO_2 with exposed {001} facets is hydro(solvo)thermal method [10, 11], and anion doped TiO_2 (e.g., N, C, S) with exposed {001} facets has been synthesized successfully by hydro(solvo)thermal method in recent years [12–14]. The resultant samples are usually with a larger size, submicron, and even several microns [15], which is disadvantaged to the photocatalytic activity of TiO_2. Therefore, anion doped TiO_2 with exposed {001} facets and smaller size is still desirable. Lots of publications have proved that sol-gel is an ideal method to prepare uniform TiO_2 powder with smaller size. Therefore, sol-gel method may be a good attempt to obtain anion doped TiO_2 nanocrystals with exposed {001} facets [16]. However, the sol-gel preparation of anion doped TiO_2 nanocrystals with exposed {001} facets has not been reported so far.

In this study, we prepared N-doped TiO_2 nanocrystals with exposed {001} facets by using sol-gel method successfully. The as-synthesized N-doped TiO_2 nanocrystals with exposed {001} facets showed higher photocatalytic activity

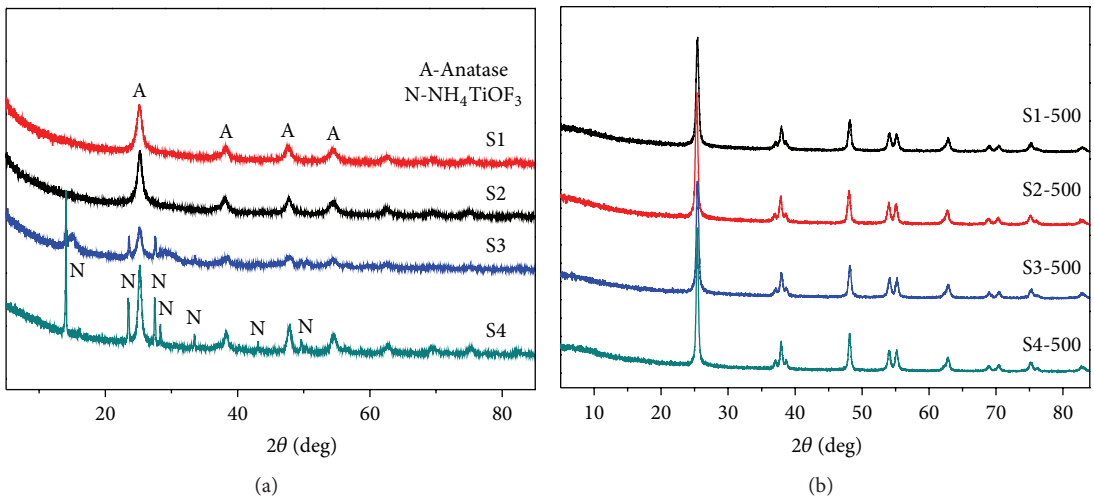

Figure 1: XRD patterns of all samples ((a) the uncalcined samples, (b) the calcined samples).

than P25 in the degradation of methylene blue (MB) dye under visible-light illumination, and the influenced factors of photocatalytic activity were discussed in detail. To our knowledge, this is the first time to prepare N-doped TiO_2 nanocrystals with exposed {001} facets successfully by using sol-gel method, and the excellent visible-light activity has rarely been reported.

2. Experimental

2.1. Preparation of N-Doped TiO_2 Nanocrystals with Exposed {001} Facets. N-doped TiO_2 nanocrystals with exposed {001} facets were synthesized by a sol-gel method [17]. Firstly, 6.85 mL of tetrabutyl titanate was dispersed in 15.5 mL of absolute ethanol under vigorous stirring for 30 min in a conical flask with cover (solution A). Secondly, a given amount of NH_4F (the molar ratio of Ti to N was controlled at 1 : 4, 1 : 2, 1 : 1, 2 : 1), 7.75 mL of absolute ethanol, 8 mL of acetic acid, and 2.88 mL of pure water were mixed in a beaker (solution B). Then, solution B was dropwise added to solution A with vigorous magnetic agitation. Subsequently, the obtained mixtures were kept in incubator chamber at 90°C for 12 h. The obtained gel from the sol-gel reaction was dried at 80°C in an oven and then porphyrized into powders. The as-obtained samples were named S1, S2, S3, and S4, respectively. In order to improve the crystallinity, the four samples were calcined at 500°C in a furnace for 2 h to obtain the samples labeled as S1-500, S2-500, S3-500, and S4-500, respectively.

2.2. Characterization. Powder X-ray diffraction (XRD) patterns were recorded at room temperature with an X'pert diffractometer (PANalytical, Holland) with copper K_{a1} radiation to determine the crystalline structure of the samples. SEM images were obtained by a field emission scanning electron microscopy (S-4800, Hitachi, Japan) equipment and TEM images were carried out on a transmission electron microscope (JEM 2100, JEOL, Japan) to characterize morphology of the samples. XPS analyses were tested on an X-ray photoelectron spectrometer (ESCALAB250, Thermo Scientific, USA) with aluminum K_a radiation to analyze the chemical nature of surface elements. UV-visible diffuse reflectance spectra (DRS) were obtained with a UV-visible spectrophotometer (UV-2450, Shimadzu, Japan) and the baseline correction was done using a standard sample of $BaSO_4$ to describe the absorption of light at different wavelengths.

2.3. Photocatalytic Performance. The photocatalytic decomposition of methylene blue (MB) was carried out in a photo reaction system (as illustrated in our previous publication [18]). The visible light source was offered by a 1000 W Xe lamp equipped with a glass filter (removing the UV irradiation below 420 nm wavelength) positioned in the center of a water-cooled system. The reactive bottle is a 50 mL cylindrical vessel 4 cm away from the light source. In the bottom of the reactive bottle, a magnetic stirrer was rotated to achieve effective dispersion. The temperature of the reaction solution was maintained at 30 ± 0.5°C by cooling water. 50 mg of samples was added to 50 mL of 10 mg/L MB solution to form suspension. After the suspensions were stirred in the dark for 1 h to reach the adsorption-desorption equilibrium, the suspensions were irradiated with visible light and stirred continuously. At given time interval, 2 mL of suspension was taken out and immediately centrifuged to eliminate the solid particles. The absorbance of the filtrate was measured by a spectrophotometer at the maximum absorbance peak 665 nm.

3. Results and Discussion

3.1. XRD. The XRD patterns of four samples are displayed in Figure 1. It can be clearly seen from Figure 1(a) the variations of products with the different dosages of NH_4F.

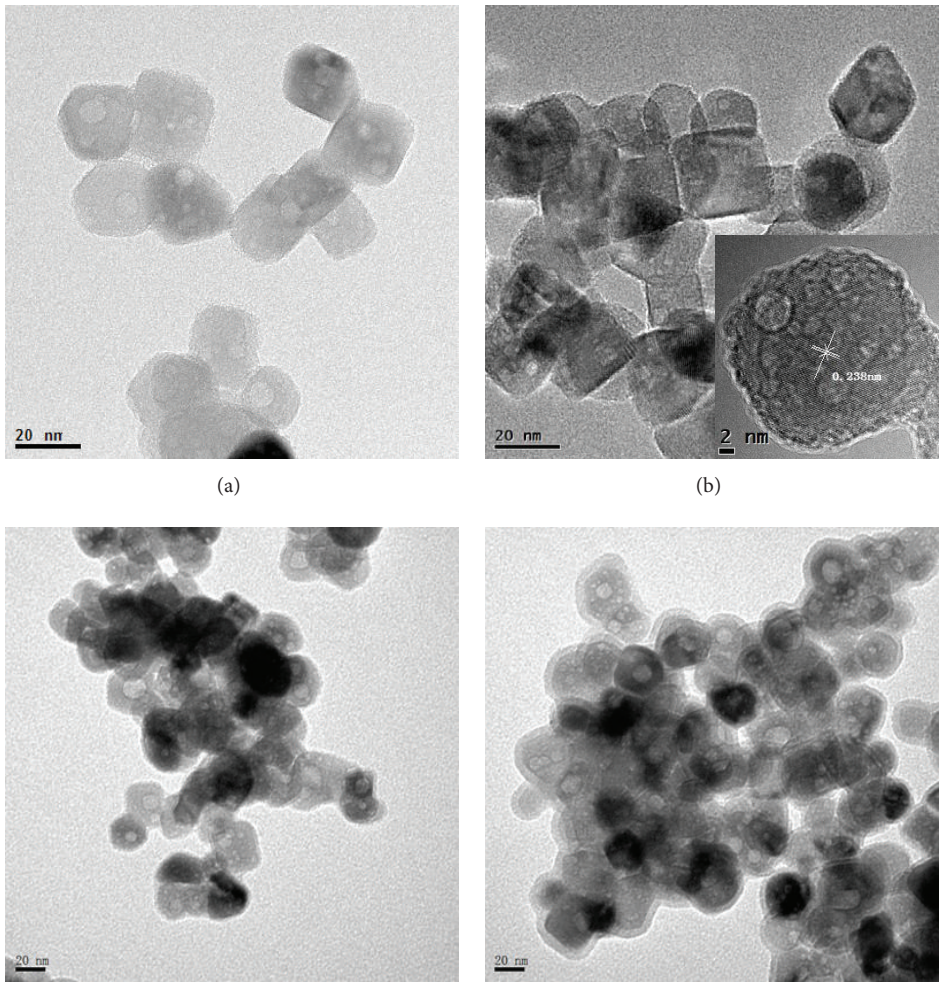

(a) (b)

(c) (d)

Figure 2: TEM pictures of all samples ((a) S1-500, (b) S2-500, (c) S3-500, and (d) S4-500).

The peaks at 2θ = 25.28°, 37.80°, 48.05°, 53.89°, 55.06°, and 62.69° belong to anatase TiO_2 (reference no. 00-021-1272), and the peaks at 2θ = 14.08°, 23.57°, 27.56°, 28.37°, 33.59°, and 49.65° are corresponding to NH_4TiOF_3 (reference no. 00-052-1674). From the contrast of four samples, we can see all the peaks of S1 and S2 belong to anatase TiO_2, indicating that only anatase TiO_2 formed when the dosages of NH_4F are relative low. With the increasing of the dosage of NH_4F, new peaks corresponding to NH_4TiOF_3 appear in the XRD patterns of S3 and S4, indicating that both anatase TiO_2 and NH_4TiOF_3 formed when the dosages of NH_4F are relative higher, and the anatase TiO_2 contents in S3 and S4 are 75.3% and 60.1%, respectively. Figure 2(b) presents the XRD patterns of the samples after calcination. Both of the two samples (S3 and S4) are transformed into anatase TiO_2 because of the heating effect. Compared with the samples without calcination treatment, the diffraction peak intensities of anatase TiO_2 are increased and the Full Width Half Maximums (FWHM) are obviously narrowed due to heat treatment, which demonstrates that the crystallization degree of anatase TiO_2 is enhanced due to the calcination at 500°C for 2 h. The average crystal size of all samples was calculated using the Scherrer equation

$$D = \frac{k\lambda}{\beta \cos\theta}, \tag{1}$$

where D is the average crystal size, k is a constant (shape factor, about 0.89), λ is the X-ray wavelength, β is the FWHM of the diffraction line, and θ is the diffraction angle. The calculated results are 16.89, 17.70, 37.73, and 25.26 nm for S1-500, S2-500, S3-500, and S4-500, respectively.

The above results can be explained by the following reasons. Because of the high hydrolytic activity of tetranbutyl titanate, it is necessary to slow down the speed of hydrolysis by adding depressor such as acetic acid. In the reaction, acetate is used as a ligand for titanium to control the rate of tetranbutyl titanate hydrolysis effectively; thus the formation of gel can be stable and controllable. Then, the coordinate

polymers are transformed into TiO_2 by condensation polymerization [16]. The followings are the reaction approaches:

$$\mathrm{Ti(OC_4H_9)_4} + n\mathrm{CH_3COOH} \longrightarrow \mathrm{Ti(OC_4H_9)_{4-n}(OOCCH_3)_n} + n\mathrm{C_4H_9OH} \quad (2)$$

$$\mathrm{Ti(OC_4H_9)_{4-n}(OOCCH_3)_n} + 4\mathrm{H_2O} \longrightarrow \mathrm{Ti(OH)_4} + (4-n)\,\mathrm{C_4H_9OH} + n\mathrm{CH_3COOH} \quad (3)$$

$$\mathrm{Ti(OH)_4} \longrightarrow \mathrm{TiO_2} + 2\mathrm{H_2O} \quad (4)$$

It is adverse to the production of TiO_2 when the dosage of NH_4F is excessive, and the reason can be ascribed to the following reactions:

$$\mathrm{NH_4F} \longrightarrow \mathrm{NH_4^+} + \mathrm{F^-} \quad (5)$$

$$\mathrm{Ti(OH)_4} + 3\mathrm{H^+} + 3\mathrm{F^-} \longrightarrow \mathrm{Ti(OH)F_3} + 3\mathrm{H_2O} \quad (6)$$

$$\mathrm{Ti(OH)F_3} + \mathrm{OH^-} + \mathrm{NH_4^+} \longrightarrow \mathrm{NH_4TiOF_3}\downarrow + \mathrm{H_2O} \quad (7)$$

3.2. TEM. Figure 2 shows the TEM images of the four calcined samples (the TEM images of uncalcined samples were not shown here due to their obscure {001} facets). As shown in Figure 2(a), when the NH_4F dosage is a quarter of titanium in amount, TiO_2 nanocrystals with the size of 15~20 nm present square outline, which is different from the morphology of TiO_2 nanocrystals prepared by traditional sol-gel method where crystal surface control agent (F^-) was absent [17], indicating the formation of nanocrystals with exposed {001} facets [19]. In Figure 2(b), TiO_2 nanocrystals show quite distinct square outline as the increasing of the dosage of NH_4F, and the nanocrystals are about 20 nm in length, about 15 nm in thickness, and about 40% in the percentage of {001} facets. When the NH_4F dosage is equal to titanium in amount, nanocrystals appear in an irregular shape and some nanocrystals are aggregated to some extent, which can be obviously seen from the TEM image (Figure 2(c)). When the NH_4F dosage is double that of the titanium, the shapes of crystals are more irregular, and the edges are obscure; the reason can be ascribed to the production of NH_4TiOF_3. That is, the anatase TiO_2 produced in the sol-gel process can likely show {001} facets after calcination. The inset in Figure 2(b) (HR-TEM of S2-500) clearly shows the continuous (004) atomic planes with a lattice spacing of 0.238 nm, corresponding to the {004} planes of anatase TiO_2 single crystals, which further confirms that the exposed crystal facet is {001} facet.

3.3. XPS. Figure 3(a) displays the XPS survey scan patterns of typical samples S2 and S2-500. Two significant differences can be observed by comparing the two samples. One of them is that the two peaks centered at 830.0 eV and 685.2 eV, which can be assigned to F (A) and F 1s, respectively, appear in uncalcined sample, and are removed due to calcination [20], indicating F groups anchored on the surface of S2 can be removed by calcinations at 500°C for 2 h. The other one is that the peak centered at about 400.0 eV is weakened, which can be ascribed to the removal of adsorbed nitrogen groups due to calcination. The small peak at about 400.0 eV in sample S2-500 can be ascribed to N 1s, implying that N-doping has been realized. As shown in Figure 3(b), two peaks can be obtained by fitting the N 1s spectrum of S2. The peak at 399.7 eV (peak 1) can be assigned to Ti-(N-O) bond [21–24], and the peak at 401.4 eV (peak 2) is attributed to the interstitial N atoms in N-O bonds [25], indicating that some nitrogen groups are adsorbed on the surface or interspace of TiO_2. In Figure 3(c), two peaks at 399.7 eV (peak 1) and 402.9 eV (peak 3) can be fitted from the N1s spectrum of S2-500, which can be assigned to Ti-(N-O) bond and O_X-Ti-N_Y bond [23, 26], implying that nitrogen atoms are doped in the lattices of TiO_2. The doping amount of nitrogen is 0.52% in atom.

3.4. DRS. Figure 4 gives the UV-Vis diffuse reflectance spectra of all samples. The optical absorption edges of S1, S2, S3, S4, and S1-500 locate at 420 nm, which is similar to pure TiO_2 (Figure 4(a)). However, the optical absorption edges of S2-500, S3-500, and S4-500 shift to the lower-energy region (about 550 nm) due to the N-doping (Figure 4(b)). These phenomena can be explained by combining UV-Vis diffuse reflectance results and XPS analysis results. Before calcination, nitrogen groups are just adsorbed on the surface or interspace of TiO_2, not doped into the lattices of TiO_2, which cannot change the band gaps of S1, S2, S3, and S4. Therefore, the optical absorption edges of the four samples do not shift towards long wavelength. After calcination, the optical absorption edge of S1-500 still locates at 420 nm, which can be ascribed to the low NH_4F dosage. The optical absorption edges of S2-500, S3-500, and S4-500 are shifted to the lower-energy region, implying that nitrogen atoms are doped into the lattices of TiO_2 due to the heat-treatment at high temperature and enough NH_4F dosage. It is widely accepted that the nitrogen incorporation into the crystal matrix of TiO_2 modifies the electronic band structure of TiO_2, leading to a new substitution N 2p band formed above O 2p valance band, which narrows the band gap of TiO_2 and shifts optical absorption to the visible light region [8, 12, 27]. In conclusion, the shift of optical absorption edge can be ascribed to the formation of impurity states in the band gap due to N-doping, which is realized by calcination treatment.

3.5. Photocatalytic Performances. Figure 5 shows the photocatalytic performance of all samples (due to low photocatalytic efficiency, the photocatalytic performances of these uncalcined samples were not shown). For comparison, P25, a standard photocatalyst, was also tested at the same conditions. From the comparison of the as-prepared four samples, it can be concluded that the photocatalytic performance of S2-500 is the optimal, and its photocatalytic performances is superior to P25 to a large extent. The high photocatalytic performance of S2-500 can be attributed to its high crystallization, better light response characteristic, and high reactivity of {001} facets.

3.5.1. Crystallization. Crystallization plays a significant role in the photocatalytic activity of TiO_2. A better crystallization

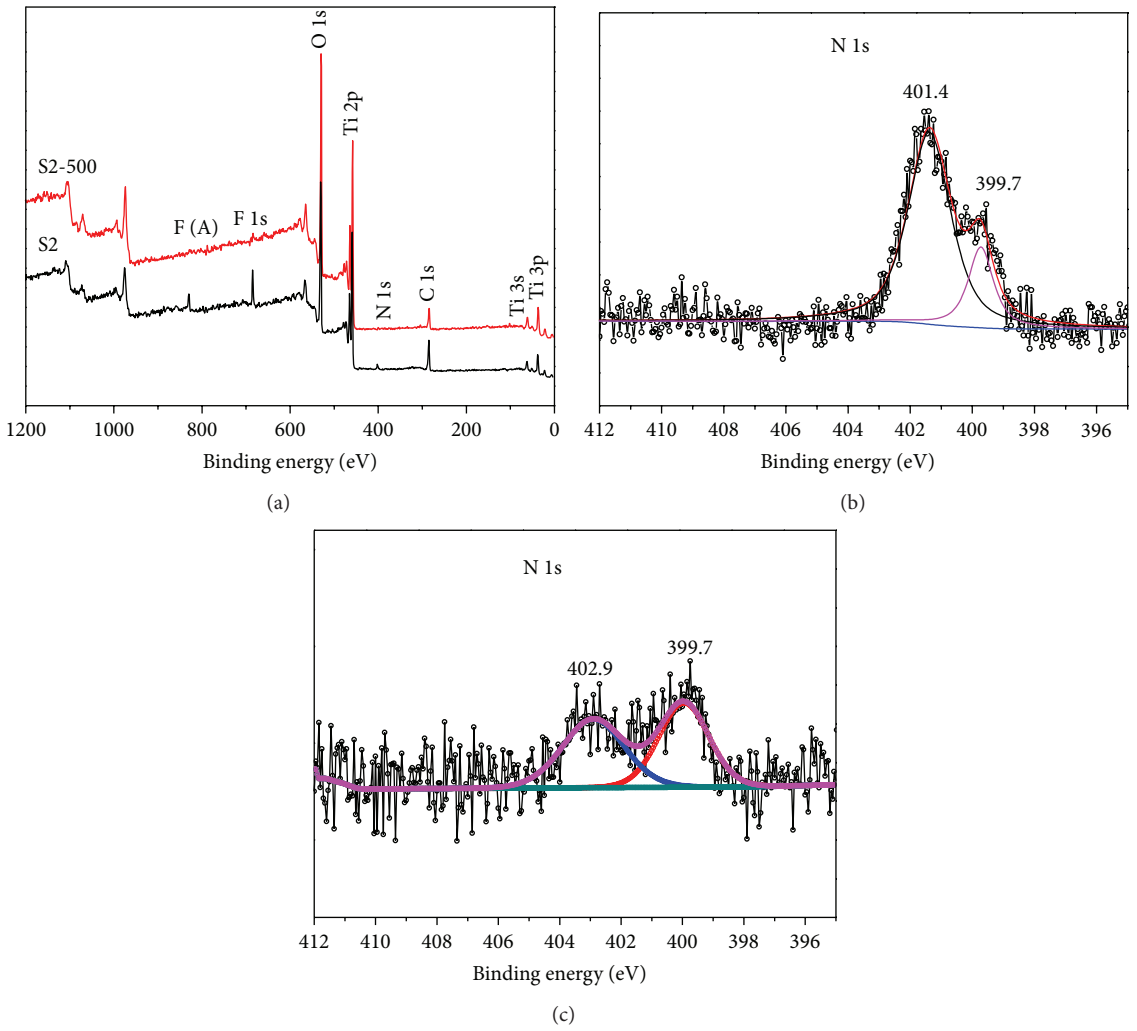

FIGURE 3: The XPS survey scan patterns of samples ((a) S2 and S2-500; (b) N 1s of S2; (c) N 1s of S2-500).

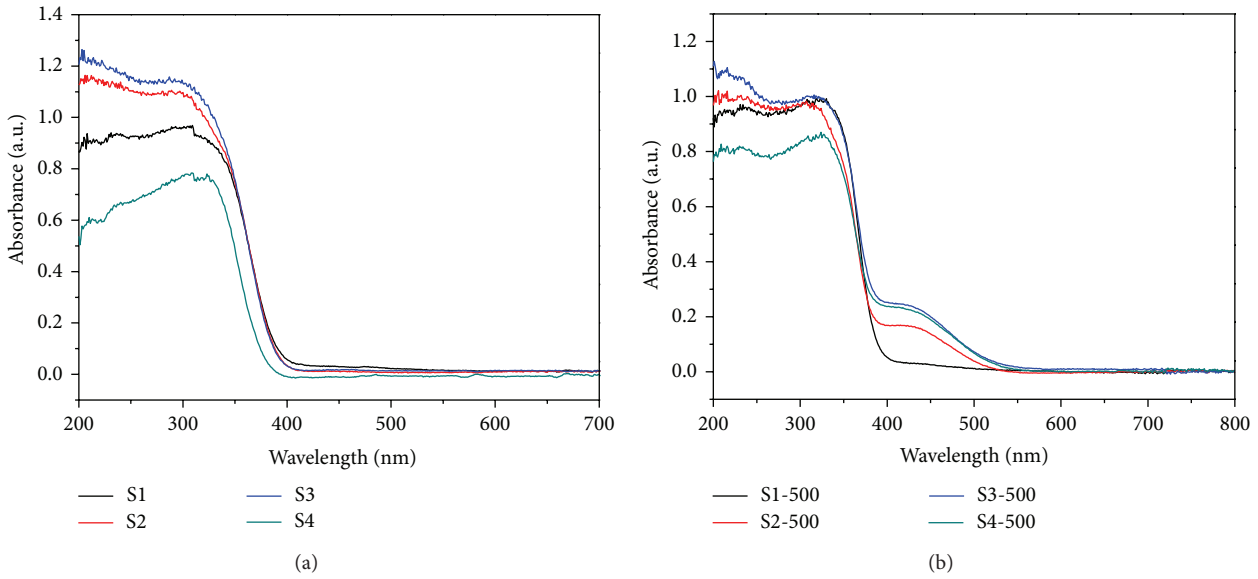

FIGURE 4: UV-Vis diffuse reflectance spectra of all samples ((a) the uncalcined samples, (b) the calcined samples).

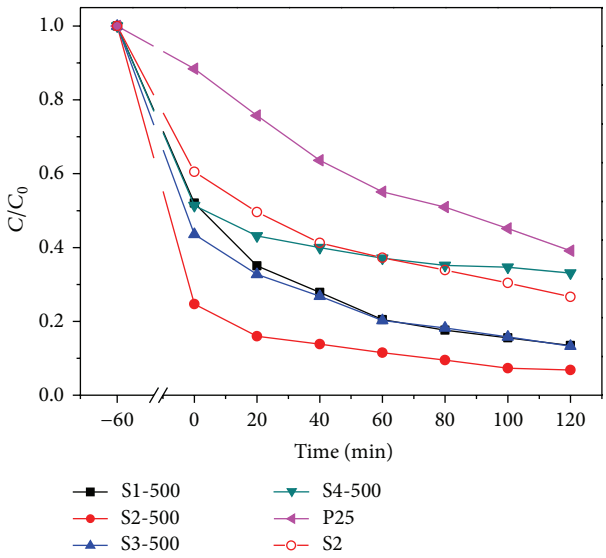

Figure 5: The photocatalytic performance of samples.

means the decrease of crystal defects, which are the recombination centers of photoinduced charges [28, 29]. Therefore, in a sense, the improvement in photocatalytic activity of TiO_2 can be achieved by increasing the crystallization of TiO_2 [30], while, heat treatment is one of the methods to improve the crystallization of TiO_2 [31, 32]. In current work, the photocatalytic performances of calcined samples are higher than those of the corresponding uncalcined samples, which can be attributed to the fact that the calcined samples possess better crystallization than the corresponding uncalcined samples, which has been confirmed from their XRD patterns.

3.5.2. Light Response Characteristic. It is well known that light absorption characteristic of photocatalyst is an important factor influencing photocatalytic activity. The enhancement of absorbance in the UV-Vis region increases the number of photogenerated electrons and holes to participate in the photocatalytic reaction, which can enhance the photocatalytic activity of TiO_2 [33, 34]. It has been confirmed from Figure 4 that the optical absorption edge of samples is shifted to 550 nm from 420 nm due to the calcination treatment, which is one of the reasons why the photocatalytic performances of calcined samples are higher than those of the corresponding uncalcined samples.

3.5.3. High Reactivity of {001} *Facets.* The surface energy of {001} facets is higher than that of {101} facets due to the 100% surface unsaturated Ti_{5C} atoms on {001} facets while only 50% for the {101} facets. Therefore, the {001} facets are theoretically considered more reactive than {101} and {010} facets [35, 36], which is in agreement with most experimental results. Under Wu's experimental conditions, the higher the percentage of {001} facets, the higher the photooxidation reactivity, for the TiO_2 crystals with the same size [6]. D'Arienzo et al. think that {001} surfaces can be considered as oxidation sites with a significant role in the photooxidation

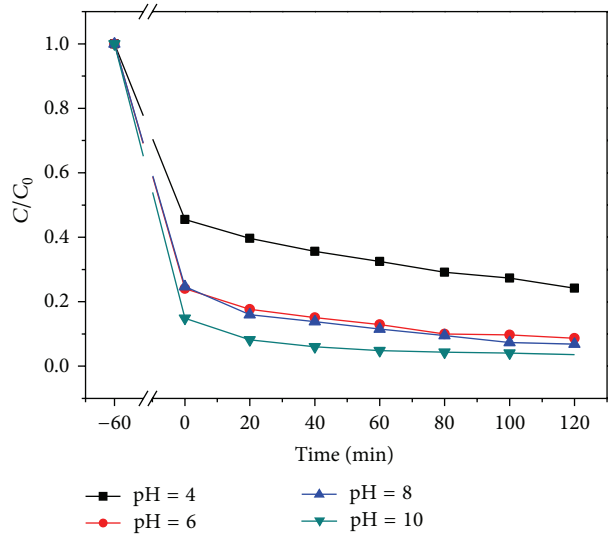

Figure 6: The effect of pH on the photocatalytic degradation efficiencies.

of TiO_2 [37]; the concentration of trapped holes (O^- centers) increases with increasing {001} surface area and photoactivity in vacuum conditions. In our experiments, the high reactivity of S2-500 can due to its high percentage of {101} facets and small size.

3.6. Factors Influencing the Photocatalytic Degradation Efficiencies. Sample S2-500 is used as the model catalyst to study the factors which influence the degradation efficiencies.

3.6.1. Effect of pH. The decoloration efficiencies of MB at different pH values are displayed in Figure 6. It shows that both the adsorption capacity and photocatalytic degradation

efficiencies will rise as pH increases. The reasons can be interpreted from the following aspects.

Firstly, pH value may influence the surface electrical behavior of TiO_2 [38]. In general, the more negative of zeta potential indicates that there are more hydroxides on the surface of TiO_2. The point of zero charge (pzc) of S2-500 is at pH 4.8; thus, the TiO_2 surface is positively charged when pH < 4.8 while it is negatively charged when pH > 4.8. It is believed that organic molecules can be adsorbed more easily onto the surface of samples with the increasing of pH.

Secondly, the changes of pH can affect the yield of $^{\bullet}OH$ radicals in the photocatalytic oxidation. The holes are considered as the major oxidation specie at low pH value whereas $^{\bullet}OH$ radicals are considered as the predominant specie at medium or high pH levels [39, 40]. It is known that $^{\bullet}OH$ radicals are easier to be generated on TiO_2 surface in alkaline environment; hence the photocatalytic activity is enhanced.

Thirdly, the stability of organic pollutants can be transformed by pH value. It is reported that MB is more stable in acid solution than that in alkaline solution [41]. Therefore, MB molecules can be degraded more easily as pH increases.

3.6.2. Effect of Catalyst Concentration. Figure 7 shows that the effect of catalyst concentration on the photocatalytic performances. It clearly displays that the adsorption capacity can be improved as the increasing of catalyst concentration. However, the photocatalytic degradation rates will not increase when the concentration exceeds a certain value. Generally, the more the dosage of catalyst, the higher the photocatalytic rate. However, excess catalysts are not favorable to boost the reaction speed for spare catalysts will shut out visible light. The optimal catalyst concentration is 1.0 $g{\cdot}L^{-1}$ in the case of our experiment condition.

3.6.3. Effect of Initial Substrate Concentration. It can be observed from Figure 8 that the photocatalytic activity of the catalyst can be influenced by substrate concentration. The degradation efficiencies decline with the increasing of substrate concentration, which can be ascribed to the following two reasons. One cause is that the generation of $^{\bullet}OH$ radicals on the surface of catalysts will be reduced because the active sites will be covered by organic ions for high substrate concentrations. Another reason is the light-screening effect of high substrate concentration, especially for dye solution; a considerable amount of light may be absorbed by dye molecules rather than TiO_2 particles, and thus it will reduce the efficiency due to the low production of $^{\bullet}OH$ radicals [42, 43].

3.6.4. Effect of Substrates. In order to confirm the universality of the catalyst, two more typical organics are used as target pollutants, namely, congo red (10 mg/L, CR) and diclofenac sodium (20 mg/L, DCF). Figure 9 shows the photocatalytic performance of S2-500 via degrading three different organic pollutants. It can be seen that the removal rates all exceed 90%. From the result, we could deduce that the synthesized nitrogen doped TiO_2 with exposed {001} facets possesses

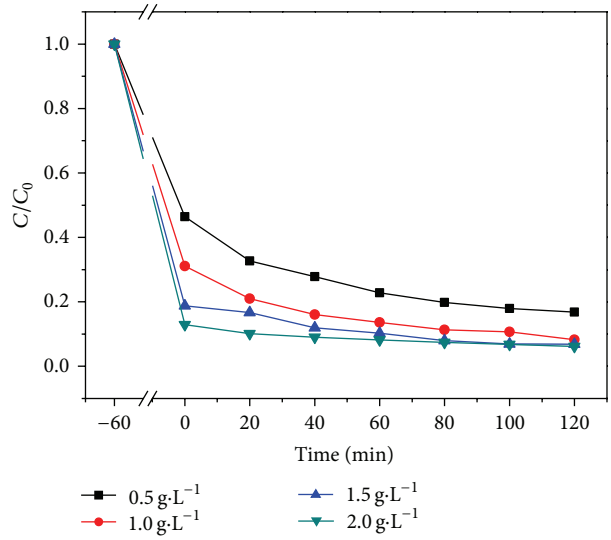

Figure 7: The effect of catalyst concentration on the photocatalytic degradation efficiencies.

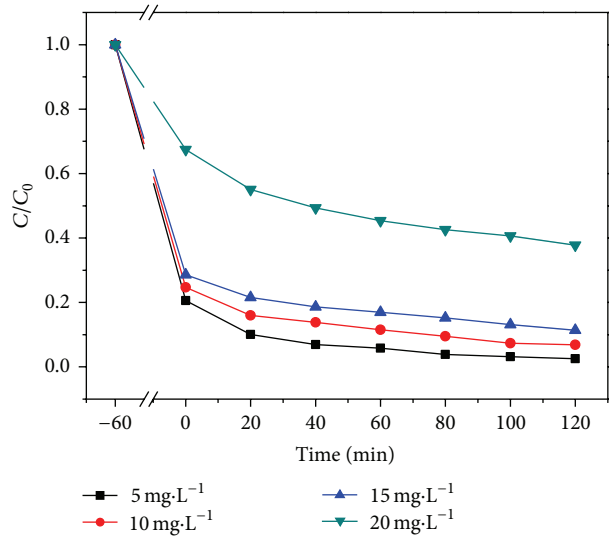

Figure 8: The effect of substrate concentration on the photocatalytic degradation efficiencies.

excellent photocatalytic performance in the degradation of organic pollutants.

4. Conclusions

In this study, nitrogen-doped TiO_2 nanocrystals with exposed {001} facets were prepared by sol-gel method firstly. The as-obtained N-doped TiO_2 nanocrystals with exposed {001} facets showed higher photocatalytic activity than P25 in the degradation of methylene blue dye under the visible-light illumination. The enhanced photocatalytic performance can be attributed to synergistic effects of several factors, such

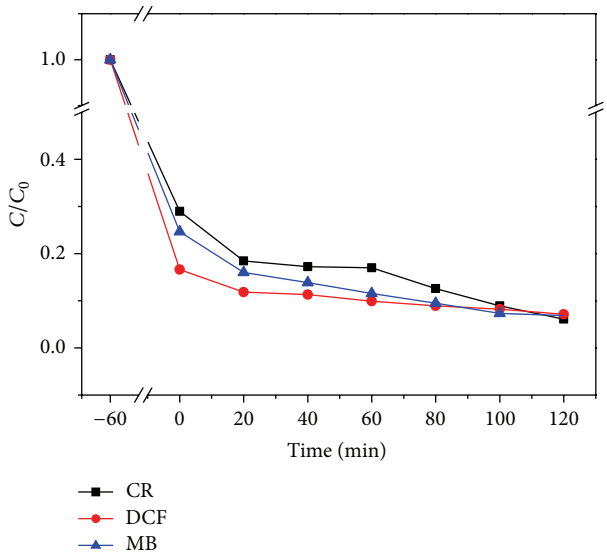

Figure 9: The photocatalytic performance of S2-500 in the degradation of different organic pollutants.

as good crystallinity, better light response characteristic, and high reactivity of {001} facets.

Conflict of Interests

The authors declare that there is no conflict of interests regarding the publishing of this paper.

Acknowledgments

This work was supported by the Key Project of Science and Technology Plan of Fujian Province (no. 2012Y0066), Xiamen Distinguished Young Scholar Award (no. 3502Z20126011), and Xiamen Science & Technology Major Program (no. 3502Z20131018). The valuable comments of anonymous reviewers are greatly appreciated.

References

[1] F. Pei, Y. Liu, S. Xu, J. Lü, C. Wang, and S. Cao, "Nanocomposite of graphene oxide with nitrogen-doped TiO_2 exhibiting enhanced photocatalytic efficiency for hydrogen evolution," *International Journal of Hydrogen Energy*, vol. 38, no. 6, pp. 2670–2677, 2013.

[2] W. Wang, C. H. Lu, Y. R. Ni, J. B. Song, M. X. Su, and Z. Z. Xu, "Enhanced visible-light photoactivity of 001 facets dominated TiO_2 nanosheets with even distributed bulk oxygen vacancy and Ti^{3+}," *Catalysis Communications*, vol. 22, pp. 19–23, 2012.

[3] D. Q. Zhang, G. S. Li, X. F. Yang, and J. C. Yu, "A micrometer-size TiO_2 single-crystal photocatalyst with remarkable 80% level of reactive facets," *Chemical Communications*, no. 29, pp. 4381–4383, 2009.

[4] H. G. Yang, C. H. Sun, S. Z. Qiao et al., "Anatase TiO_2 single crystals with a large percentage of reactive facets," *Nature*, vol. 453, no. 7195, pp. 638–641, 2008.

[5] T. R. Gordon, M. Cargnello, T. Paik et al., "Nonaqueous synthesis of TiO_2 nanocrystals using TiF4 to engineer morphology, oxygen vacancy concentration, and photocatalytic activity," *Journal of the American Chemical Society*, vol. 134, no. 15, pp. 6751–6761, 2012.

[6] Q. Wu, M. Liu, Z. Wu, Y. Li, and L. Piao, "Is photooxidation activity of 001 facets truly lower than that of 101 facets for anatase TiO2 crystals?" *The Journal of Physical Chemistry C*, vol. 116, no. 51, pp. 26800–26804, 2012.

[7] N. Serpone, "Is the band gap of pristine TiO_2 narrowed by anion- and cation-doping of titanium dioxide in second-generation photocatalysts?" *Journal of Physical Chemistry B*, vol. 110, no. 48, pp. 24287–24293, 2006.

[8] R. Asahi, T. Morikawa, T. Ohwaki, K. Aoki, and Y. Taga, "Visible-light photocatalysis in nitrogen-doped titanium oxides," *Science*, vol. 293, no. 5528, pp. 269–271, 2001.

[9] D. Jing, S. Yao, P. Chen et al., "A multichannel system for rapid determination of the activity for photocatalytic H_2 production," *AIChE Journal*, vol. 58, no. 11, pp. 3593–3596, 2012.

[10] H. Zhang, X. Liu, Y. Li, and H. Zhao, "001 facets dominated anatase TiO_2: morphology, formation/etching mechanisms and performance," *Science China Chemistry*, vol. 56, no. 4, pp. 402–417, 2013.

[11] H. G. Yang, G. Liu, S. Z. Qiao et al., "Solvothermal synthesis and photoreactivity of anatase TiO_2 nanosheets with dominant 001 facets," *Journal of the American Chemical Society*, vol. 131, no. 11, pp. 4078–4083, 2009.

[12] G. Liu, G. Y. Hua, X. Wang et al., "Visible light responsive nitrogen doped anatase TiO_2 sheets with dominant 001 facets derived from TiN," *Journal of the American Chemical Society*, vol. 131, no. 36, pp. 12868–12869, 2009.

[13] J. Yu, G. Dai, Q. Xiang, and M. Jaroniec, "Fabrication and enhanced visible-light photocatalytic activity of carbon self-doped TiO_2 sheets with exposed 001 facets," *The Journal of Physical Chemistry C*, vol. 21, no. 4, pp. 1049–1057, 2011.

[14] G. Liu, C. Sun, S. C. Smith, L. Wang, G. Q. M. Lu, and H. M. Cheng, "Sulfur doped anatase TiO_2 single crystals with a high percentage of 001 facets," *Journal of Colloid and Interface Science*, vol. 349, no. 2, pp. 477–483, 2010.

[15] G. Liu, J. C. Yu, G. Q. Lu, and H.-M. Cheng, "Crystal facet engineering of semiconductor photocatalysts: motivations, advances and unique properties," *Chemical Communications*, vol. 47, no. 24, pp. 6763–6783, 2011.

[16] K. Terabe, K. Kato, H. Miyazaki, S. Yamaguchi, A. Imai, and Y. Iguchi, "Microstructure and crystallization behaviour of TiO_2 precursor prepared by the sol-gel method using metal alkoxide," *Journal of Materials Science*, vol. 29, no. 6, pp. 1617–1622, 1994.

[17] J. Shi, S. Chen, S. Wang, and Z. Ye, "Sol-gel preparation and visible light photocatalytic activity of nitrogen doped titania," *Procedia Engineering*, vol. 27, pp. 564–569, 2012.

[18] J. Shi, X. Zong, X. Wu et al., "Carbon-doped titania hollow spheres with tunable hierarchical macroporous channels and enhanced visible light-induced photocatalytic activity," *ChemCatChem*, vol. 4, no. 4, pp. 488–491, 2012.

[19] L. Sun, Z. Zhao, Y. Zhou, and L. Liu, "Anatase TiO_2 nanocrystals with exposed heets via molecular grafting for enhanced photocatalytic activity," *Nanoscale*, vol. 4, no. 2, pp. 613–620, 2012.

[20] X. Zhou, F. Peng, H. Wang, H. Yu, and Y. Fang, "A simple preparation of nitrogen doped titanium dioxide nanocrystals with exposed (001) facets with high visible light activity," *Chemical Communications*, vol. 48, no. 4, pp. 600–602, 2012.

[21] Y. Cong, J. Zhang, F. Chen, and M. Anpo, "Synthesis and characterization of nitrogen-doped TiO_2 nanophotocatalyst with high visible light activity," *The Journal of Physical Chemistry C*, vol. 111, no. 19, pp. 6976–6982, 2007.

[22] E. György, A. Pérez del Pino, P. Serra, and J. L. Morenza, "Depth profiling characterisation of the surface layer obtained by pulsed Nd:YAG laser irradiation of titanium in nitrogen," *Surface and Coatings Technology*, vol. 173, no. 2-3, pp. 265–270, 2003.

[23] C. Chen, H. Bai, and C. Chang, "Effect of plasma processing gas composition on the nitrogen-doping status and visible light photocatalysis of TiO_2," *The Journal of Physical Chemistry C*, vol. 111, no. 42, pp. 15228–15235, 2007.

[24] R. Asahi and T. Morikawa, "Nitrogen complex species and its chemical nature in TiO_2 for visible-light sensitized photocatalysis," *Chemical Physics*, vol. 339, no. 1–3, pp. 57–63, 2007.

[25] C. S. Gopinath, "Comment on 'photoelectron spectroscopic investigation of nitrogen-doped titania nanoparticles'," *Journal of Physical Chemistry B*, vol. 110, no. 13, pp. 7079–7080, 2006.

[26] N. Yang, G. Li, W. Wang, X. Yang, and W. F. Zhang, "Photophysical and enhanced daylight photocatalytic properties of N-doped TiO_2/g-C_3N_4 composites," *Journal of Physics and Chemistry of Solids*, vol. 72, no. 11, pp. 1319–1324, 2011.

[27] H. Irie, S. Washizuka, N. Yoshino, and K. Hashimoto, "Visible-light induced hydrophilicity on nitrogen-substituted titanium dioxide films," *Chemical Communications*, vol. 9, no. 11, pp. 1298–1299, 2003.

[28] J. Yu, G. Wang, B. Cheng, and M. Zhou, "Effects of hydrothermal temperature and time on the photocatalytic activity and microstructures of bimodal mesoporous TiO_2 powders," *Applied Catalysis B: Environmental*, vol. 69, no. 3-4, pp. 171–180, 2007.

[29] M. Mrowetz, W. Balcerski, A. J. Colussi, and M. R. Hoffmann, "Oxidative power of nitrogen-doped TiO_2 photocatalysts under visible illumination," *The Journal of Physical Chemistry B*, vol. 108, no. 45, pp. 17269–17273, 2004.

[30] J. Ovenstone, "Preparation of novel titania photocatalysts with high activity," *Journal of Materials Science*, vol. 36, no. 6, pp. 1325–1329, 2001.

[31] H. Wang, Y. Wu, and B.-Q. Xu, "Preparation and characterization of nanosized anatase TiO_2 cuboids for photocatalysis," *Applied Catalysis B: Environmental*, vol. 59, no. 3-4, pp. 139–146, 2005.

[32] M. Salmi, N. Tkachenko, V. Vehmanen, R. Lamminmäki, S. Karvinen, and H. Lemmetyinen, "The effect of calcination on photocatalytic activity of TiO_2 particles: femtosecond study," *Journal of Photochemistry and Photobiology A: Chemistry*, vol. 163, no. 3, pp. 395–401, 2004.

[33] D. Li, H. Haneda, S. Hishita, and N. Ohashi, "Visible-light-driven nitrogen-doped TiO_2 photocatalysts: effect of nitrogen precursors on their photocatalysis for decomposition of gas-phase organic pollutants," *Materials Science and Engineering B*, vol. 117, no. 1, pp. 67–75, 2005.

[34] M. Hamadanian, A. Reisi-Vanani, and A. Majedi, "Synthesis, characterization and effect of calcination temperature on phase transformation and photocatalytic activity of Cu, S-codoped TiO_2 nanoparticles," *Applied Surface Science*, vol. 256, no. 6, pp. 1837–1844, 2010.

[35] A. Selloni, "Crystal growth: anatase shows its reactive side," *Nature Materials*, vol. 7, no. 8, pp. 613–615, 2008.

[36] X. Gong and A. Selloni, "Reactivity of anatase TiO_2 nanoparticles: the role of the minority (001) surface," *The Journal of Physical Chemistry B*, vol. 109, no. 42, pp. 19560–19562, 2005.

[37] M. D'Arienzo, J. Carbajo, A. Bahamonde et al., "Photogenerated defects in shape-controlled TiO_2 anatase nanocrystals: a probe to evaluate the role of crystal facets in photocatalytic processes," *Journal of the American Chemical Society*, vol. 133, no. 44, pp. 17652–17661, 2011.

[38] M. A. Fox and M. T. Dulay, "Heterogeneous photocatalysis," *Chemical Reviews*, vol. 93, no. 1, pp. 341–357, 1993.

[39] L. Lucarelli, V. Nadtochenko, and J. Kiwi, "Environmental photochemistry: quantitative adsorption and FTIR studies during the TiO_2-photocatalyzed degradation of orange II," *Langmuir*, vol. 16, no. 3, pp. 1102–1108, 2000.

[40] W. Z. Tang and C. P. Huang, "Photocatalyzed oxidation pathways of 2,4-dichlorophenol by CdS in basic and acidic aqueous solutions," *Water Research*, vol. 29, no. 2, pp. 745–756, 1995.

[41] N. Bélaz-David, L. A. Decosterd, M. Appenzeller et al., "Spectrophotometric determination of methylene blue in biological fluids after ion-pair extraction and evidence of its adsorption on plastic polymers," *European Journal of Pharmaceutical Sciences*, vol. 5, no. 6, pp. 335–345, 1997.

[42] I. K. Konstantinou and T. A. Albanis, "TiO_2-assisted photocatalytic degradation of azo dyes in aqueous solution: kinetic and mechanistic investigations: a review," *Applied Catalysis B: Environmental*, vol. 49, no. 1, pp. 1–14, 2004.

[43] N. Daneshvar, D. Salari, and A. R. Khataee, "Photocatalytic degradation of azo dye acid red 14 in water: investigation of the effect of operational parameters," *Journal of Photochemistry and Photobiology A: Chemistry*, vol. 157, no. 1, pp. 111–116, 2003.